*Korean J. Chem. Eng.*, 34(9), 2459-2470 (2017)
DOI: 10.1007/s11814-017-0152-8

pISSN: 0256-1115
eISSN: 1975-7220

# Synthesis and characterization of poly(ether-*block*-amide) copolymers/multi-walled carbon nanotube nanocomposite membranes for $CO_2/CH_4$ separation

**Navid Azizi, Mehran Arzani, Hamid Reza Mahdavi, and Toraj Mohammadi†**

Research and Technology Center of Membrane Processes, Chemical Engineering Department,
Iran University of Science and Technology (IUST), Narmak, Tehran, Iran
(*Received 12 April 2017 • accepted 29 May 2017*)

**Abstract**−One of the effective techniques for improving separation properties of polymeric membranes is incorporation of suitable nanoparticles into their matrices. This study presents the preparation of three types of nanocomposite membranes comprising three grades of poly (ether-*block*-amide) (Pebax 1074, Pebax 1657 and Pebax 2533) and modified multi-walled carbon nanotubes (MWCNTs) with different loadings (1, 1.5, 2 and 2.5 wt%). The prepared membranes were characterized by field emission scanning electron microscopy (FESEM), attenuated total reflection-Fourier transfer infrared spectroscopy (ATR-FTIR) and X-ray diffraction (XRD). Permeation of $CO_2$ and $CH_4$ gases through the prepared membranes was measured at the pressure range of 2-8 bars and 25 °C. The results showed that the incorporation of MWCNTs into the polymers matrices improves $CO_2/CH_4$ selectivity. Further, Pebax 1074/MWCNT nanocomposite membrane exhibits better performance for $CO_2/CH_4$ separation compared to the neat Pebax and the two other nanocomposite membranes.

Keywords: Pebax, Nanocomposite Membranes, Multi-walled Carbon Nanotubes, Gas Separation

## INTRODUCTION

Membrane processes have attracted much interest in natural gas sweetening and environmental pollutants removal compared to other common separation methods [1,2]. Being less expensive and more flexible, occupying lower space, and consuming less power can be noted as the advantages of membrane processes [3-6]. In the past twenty years, several polymeric membranes have been used for separation of gas mixtures, and numerous studies have been reported. Robeson collected some information about the properties of polymeric membranes in terms of selectivity-permeability figures for various gas pairs and presented the upper bound limits for their performance [7-10]. Since polymeric membranes with high gas separation efficiencies can be applied in gas separation industries, their performance should be improved. One way to improve gas transport properties of polymeric membranes is the incorporation of nanoparticles in polymer matrices as a solution for overcoming Robeson trade-off limits [11-13].

Polymers with ether oxygen units (EO) in their structures can interact better with polar gases like $CO_2$ and consequently $CO_2$ solubility in the prepared membranes of such polymers is higher. Thus, it is expected to have higher separation performance for $CO_2$/non-polar gases [14]. Co-polymers such as Pebax are commercial thermoplastics that have been used in various gas separations. It contains polyether (PE) and polyamide (PA) segments. Various properties of different Pebax grades depend on the segment amounts. PE is the soft segment which is responsible for penetrant permeability through the prepared membrane and its chain flexibility, while PA block is the hard segment applied to supply its mechanical strength. As mentioned earlier, incorporation of inorganic fillers into polymeric membranes is an efficient way to improve their gas separation properties [15,16]. A variety of fillers such as non-porous (metal oxides and clay) and porous ones (zeolites, carbon molecular sieves and carbon nanotubes) have been employed for this purpose [17-20]. MWCNTs have been attracted much research interest due to their porous structure, high adsorption capacity and good thermal, mechanical and electrical properties. Many researches have been conducted to study adsorption capacity of MWCNTs. The results showed that it has more affinity for $CO_2$ compared to non-polar gases. Zhao et al. [1] investigated adsorption capacity of MWCNTs for $CO_2$, $CH_4$ and $N_2$ gases. The obtained results confirmed more $CO_2$ adsorption tendency of MWCNTs compared to the other gases. Recently, Molyanyan et al. [21] also studied $CO_2$ and $CH_4$ adsorption on MWCNTs. The results showed that capacity of MWCNTs for $CO_2$ adsorption is higher than that for $CH_4$. Several studies have been carried out on incorporating of MWCNTs into different Pebax grades, as can be seen in Table 1. However, there is no evidence in investigating effect of MWCNTs addition on different Pebax grades, simultaneously. Different parameters can affect the performance of the prepared membranes such as time and temperature of drying, solvent type, etc. Since these parameters are variable in various published researches, one may not be able to distinguish which grade of Pebax is more effective for preparation of Pebax/MWCNT membranes. As a result, our objective was to fix those parameters and only change the Pebax grade for this purpose. Therefore, in the present work, the nanocomposite membranes using different grades of Pebax (1074, 1657 and 2533) as the basic polymer matrix and different contents of MWCNTs

†To whom correspondence should be addressed.
E-mail: torajmohammadi@iust.ac.ir

**Table 1. Different studies on application of MWCNTs in different grades of Pebax**

| Polymer matrix | Types of gas mixture | Result | Ref. |
|---|---|---|---|
| Pebax 1074 | $CO_2$ and $N_2$ | The results demonstrated a 40% $CO_2$ permeability increase | [54] |
| Pebax 1657 | $CO_2$, $H_2$, $N_2$ and $CH_4$ | By 33 wt% nanoparticles loading, $CO_2$ permeability grew around 3 times. The selectivities of $CO_2/N_2$, $CO_2/H_2$ and $CO_2/CH_4$ were not changed considerably | [1] |
| Pebax 1657 | $CO_2$, $H_2$, $N_2$, and $O_2$ | $CO_2/N_2$ and $CO_2/H_2$ selectivities were enhanced by mixing 2 wt% nanoparticles loading | [34] |
| Pebax 1657 | $CO_2$, $H_2$ and $N_2$ | $CO_2$ permeability and the mechanical strength were promoted. Also, $CO_2/N_2$ and $CO_2/H_2$ selectivity remained nearly constant | [41] |
| Pebax 1657/PEG | $CO_2$ and $CH_4$ | The higher content of nanoparticles is, the increasing $CO_2$ permeability will be. Besides, no significant change in the $CO_2/CH_4$ selectivity was observed | [48] |
| Pebax 1657/PEG | $CO_2$, $N_2$ and $CH_4$ | $CO_2$ permeability was increased, whereas a slight decrease in $CO_2/CH_4$ selectivity was seen. But, $CO_2/N_2$ selectivity was increased | [46] |

**Table 2. Physical properties of different grades of Pebax**

| Property | Pebax 1074 | Pebax 1657 | Pebax 2533 | Unit |
|---|---|---|---|---|
| PE content | 55 | 60 | 80 | wt% |
| Density | 1.07 | 1.14 | 1 | $g/cm^3$ |
| Water absorption at 23 °C and 24 h in water | 48 | 120 | 1.2 | wt% |
| Melting point | 158 | 204 | 134 | °C |
| Glass transition temperature | −55 | −56 | −65 | °C |
| Stress at break | 30 | 32 | 32 | MPa |

(1, 1.5, 2 and 2.5 wt%) as the filler were investigated. Permeation values of $CO_2$ and $CH_4$ gases through all the prepared membranes were measured using a constant pressure apparatus at temperature of 25 °C and pressures of 2, 4, 6 and 8 bar to evaluate their separation properties. Additionally, the prepared membranes were characterized using XRD, ATR-FTIR and FESEM analysis to examine the influence of MWCNTs loading on crystalline structures, chemical bonds and morphologies of the prepared membranes, respectively.

## EXPERIMENTAL

### 1. Materials

Elliptic pellets of Pebax 1074, Pebax 1657 and Pebax 2533 were purchased from Arkema Inc. Their physical properties are presented in Table 2. Multi-walled carbon nanotubes (MWCNTs) (inner diameter 3-6 nm, outer diameter 8-15 nm, purity >90%) were supplied from US Research Nanomaterials. Dimethylformamide (DMF) as the solvent for the membrane preparation and nitric acid ($HNO_3$, 65%) and sulfuric acid ($H_2SO_4$, 95-97%) as modifying agents for the nanoparticles treatment were supplied by Merck. Water used in MWCNTs functionalization was deionized using a Milli-Q water purification system (Millipore Corp). Research grade gases of $CO_2$ and $CH_4$ were bought from Farafan Gas Company.

### 2. MWCNTs Functionalization

Strong inter-tube van der Waals interactions of MWCNTs lead to its insolubility in all solvents and therefore sedimentation and agglomeration [22]. Covalent functionalization is one of the common methods used to prevent the nanoparticles from these phenomena [23]. Incorporation of functional groups onto MWCNTs can cause their better distribution into a polymer due to the reduced surface energies difference between the nanoparticles and the polymer. Thus, when functionalized MWCNTs are used as inorganic compounds for nanocomposite membranes preparation, the dispersion is very desirable and nanoparticle sedimentation and agglomeration are mostly avoided. For MWCNTs functionalization, 0.2 gr of pure MWCNTs was immersed in 100 ml solution of $HNO_3$ and $H_2SO_4$ with 1 and 3 $mol \cdot lit^{-1}$, respectively. This solution was refluxed at 140 °C for 3 h. The oxidized MWCNTs was then washed using deionized water several times up to neutral pH, and then the product was dried at 80 °C for 6 h [24].

### 3. Membrane Preparation

The polymers should become free of moisture before using; therefore, for this purpose, all grades of Pebax were placed in a vacuum oven at 80 °C for 6 h. For the preparation of the neat membranes, first, certain amounts (4 wt%) of three grades of polymers were added into DMF, separately. Then, the mixtures of polymers and DMF were put in three oil baths with different temperatures (105, 115, and 80 °C for Pebax 1074, Pebax 1657 and Pebax 2533, respectively) and stirred for 3 h using three magnetic stirrers. After complete dissolving of the polymers granules in the solvent, the solutions were cast into glass Petri-dishes. All samples were kept in an oven at 50 °C for 14 h. Thereafter, the samples were removed from the Petri-dishes slowly and placed in a desiccator until usage [25,26].

For synthesis of the nanocomposite membranes with the modified MWCNTs, the following procedure was carried out. First, a certain amount of the surface modified MWCNTs (1, 1.5, 2, and 2.5 wt%) was added into DMF. Then, the mixture was sonicated using a powerful probe sonicator for 30 min. The mixture was then put in an oil bath whose temperature was set at the solving temperature of the polymer, and Pebax granules were added into the

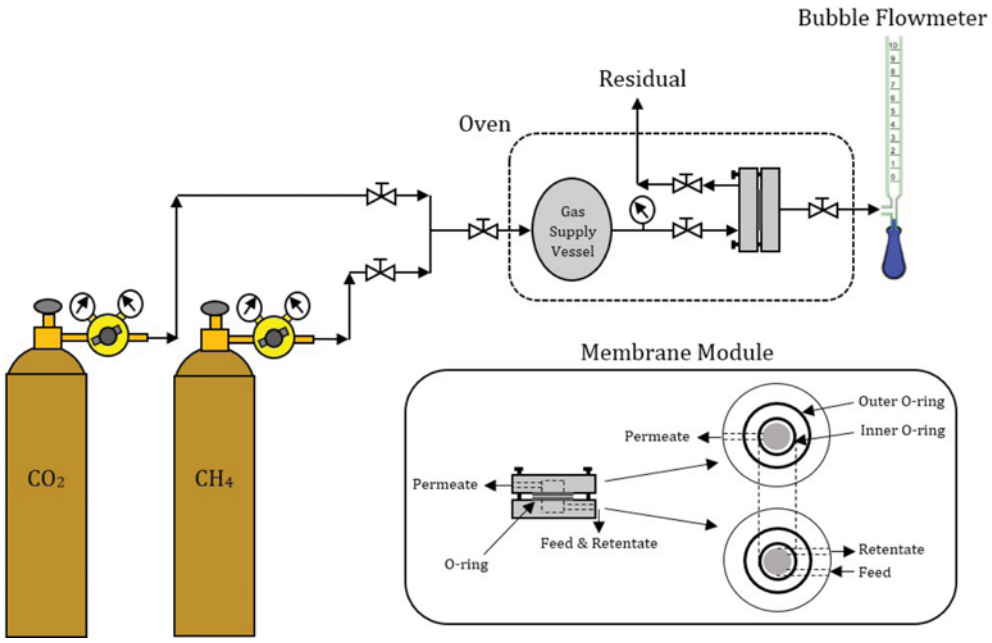


**Fig. 1. Schematic view of the setup and the module used to perform gas permeation experiments.**

mixture in several steps for priming the MWCNTs with the polymer, resulting in better interaction between the polymer and the nanoparticles and accordingly better dispersion of the MWCNTs in the mixture. After the polymer granules were completely dissolved in DMF, the solution was further sonicated for 5 min for better distribution of the MWCNTs in the polymer matrix. Finally, the casting and drying procedures applied to the neat membranes followed. The thickness of the prepared films measured using a digital micrometer was between 50 and 70 μm.

**4. Membrane Characterization**

4-1. X-ray Diffraction (XRD)

X-ray diffraction measurements were carried out using a JEOL, JDX-8030 diffractometer (XRD). The angle ($2\theta$) of diffraction was varied from 5 to 70 to identify crystal structure and intermolecular distances between the intersegment chains. The X-rays of 1.5406 A° wavelength was generated by a Cu K$\alpha$ source.

4-2. Attenuated Total Reflection-Fourier Transfer Infrared Spectroscopy (ATR-FTIR)

Fourier transform infrared spectroscopy (FTIR) was performed via Shimadzu 8400S spectrometer equipped with attenuated total reflectance (ATR) accessory. All spectra were acquired from 4,000 to 400 $cm^{-1}$ under ambient conditions on wafers consisting of 100 mg dry KBr and about 1 mg sample, with a spectral resolution of 2 $cm^{-1}$.

4-3. Field Emission Scanning Electron Microscopy (FESEM)

Morphology of the membranes was studied using field emission scanning electron microscopy (FESEM). FESEM analysis involved a JEOL, JSM-7600F. The samples were fractured in liquid nitrogen, then coated with gold and finally observed.

**5. Gas Permeation Measurements**

To measure gases ($CO_2$ and $CH_4$) permeations through the prepared membranes, an experimental setup was designed and constructed [27]. The membrane module included two detachable parts made from stainless steel (grade 316) in the cross-flow. The membranes were put in the module and, in order to provide a pressure tight seal between the membranes and the module, two rubber O-rings were used. The membrane effective diameter was about 5.2 cm. Schematic view of the setup and the module is shown in Fig. 1.

All the experiments were carried out via the constant pressure method. The pure gases were fed into the module at certain pressures (2, 4, 6 and 8 bar), which could be fixed using a pressure regulator, while the permeate side was adjusted at atmospheric pressure. The feed temperature remained constant at 25 °C for all the experiments. Volumetric flow rate of the permeate gas was measured by a bubble flow meter. After steady state was reached (2 h), the gases permeabilities were calculated using the following equation [28]:

$$P_i = \frac{Q_i \times l}{A \times (p_f - p_p)} \quad (1)$$

where, $P_i$, $Q_i$, $l$, A, $p_f$ and $p_p$ are the gas permeability expressed in Barrer (1 Barrer=$10^{-10}$ $cm^3$ (STP) cm·$cm^{-2}$·$s^{-1}$·$cmHg^{-1}$), flow rate of the permeate gas through the membrane ($cm^3$ (STP)/s), the membrane thickness (cm), the membrane effective area ($cm^2$), the absolute feed side pressure (cmHg) and the absolute permeate side pressure (cmHg), respectively.

The ideal selectivity of gases 'i and j' ($\alpha_{ij}$) for the membranes was calculated using the pure gas permeability values as follows [29]:

$$\alpha_{ij} = \frac{P_i}{P_j} \quad (2)$$

## RESULTS AND DISCUSSION

**1. Membrane Characterization**

1-1. XRD

To understand gas permeability and selectivity behavior of poly-

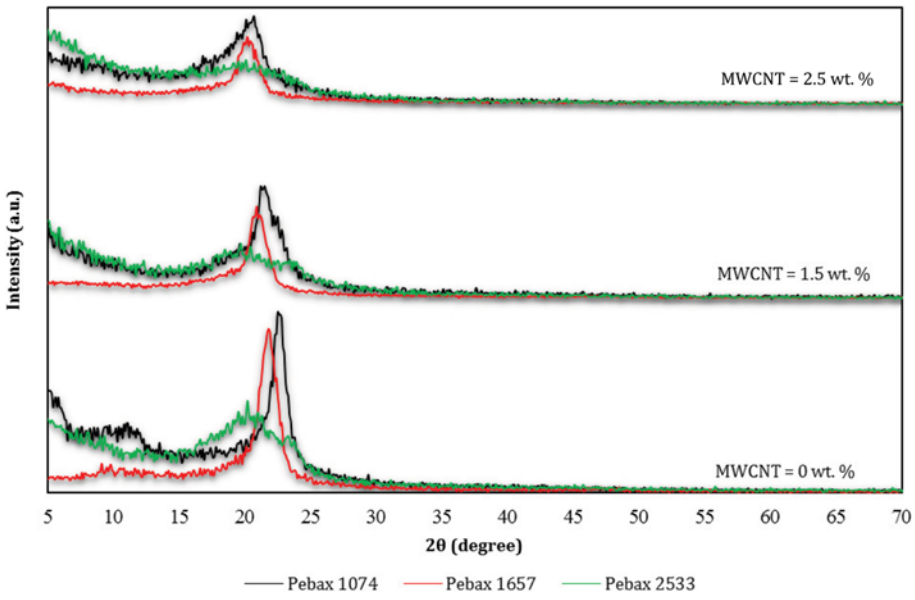


**Fig. 2. XRD patterns of the fabricated membranes with different grades of Pebax and different loadings of MWCNTs.**

meric membranes, knowing their crystalline structures via XRD analysis is necessary [30]. XRD patterns of the fabricated membranes with different grades of Pebax and different amounts of MWCNTs are presented in Fig. 2. Different Pebax grades are semi-crystalline polymers and own strong diffraction peaks related to their PA crystalline regions and weak diffraction peaks related to their PE crystalline regions. The diffraction peaks' intensities and their positions depend on their amorphous and crystalline natures [31]. As shown in Fig. 2, fabricated Pebax 1074, Pebax 1657 and Pebax 2533 membranes indicate strong diffraction peaks at 22.5°, 21.8° and 20.2°, respectively. These diffraction peaks are related to the PA region. Whereas, the diffraction peaks related to the PE region in Pebax 1074 and Pebax 1657 are at 10.9° and 9.8°, respectively. However, no diffraction peak related to the PE region of Pebax 2533 can be observed in Fig. 2. Since three grades of Pebax are different in amounts of the PE segment, it is expected to have different crystallinity for these types of Pebax [32,33]. As illustrated in Fig. 2, for the neat membranes (MWCNTs=0 wt%), with increasing the PE segment (55, 60 and 80 for Pebax 1074, Pebax 1657 and Pebax 2533, respectively) their crystallinity decreases as the crystalline peaks intensities decreases. Thus, the order of crystallinity is as follows:

Pebax 1074>Pebax 1657>Pebax 2533.

In addition to the polymer crystallinity, position of the crystalline peaks is significant for determination of permeation properties of the membranes. Generally, the reduction in $2\theta$ values increases the d-spacing (d) values based on the Bragg's equation ($n\lambda = 2d\sin\theta$). D-spacing is a measure of molecule distance between polymer chains. The greater the value of d-spacing, the higher tendency of gas molecule transport [1,33]. In accordance with the peak position of the different grades of Pebax, the order of d-spacing value is as follows:

Pebax 2533>Pebax 1657>Pebax 1074.

As discussed, it is expected that Pebax 2533 membrane exhibits the best gas permeation values compared to the two other membranes.

Generally speaking, incorporation of nanoparticles into a polymer matrix can change the degree of crystallinity of the prepared nanocomposite membranes. As can be seen in XRD patterns of the fabricated nanocomposite membranes (MWCNT=1.5 wt% and MWCNT=2.5 wt%), the addition of MWCNTs leads to the membrane crystallinity reduction due to the cohesive energy and interchain hydrogen bonding decrements between PA segments. Besides, the peaks' positions move to the lower $2\theta$ values [34].

Comparison of XRD patterns of the three types of nanocomposite membranes revealed that the order of crystallinity and d-spacing are similar to the neat membranes. Therefore, similar trends for gas permeability through the nanocomposite membranes are expected. Moreover, MWCNTs addition affects Pebax 1074 more than two other Pebax based membranes. In other words, intensities and positions of the crystalline peaks in Pebax 1074 change more because it contains the higher content of PA blocks, which are connected by interchain hydrogen bondings and accordingly addition of MWCNTs can disturb these bondings more. Besides, the higher the content of MWCNTs in the polymers matrices, the more significant the changes in crystallinities of the polymeric nanocomposite membranes.

1-2. FTIR and ATR-FTIR

1-2-1. MWCNTs FTIR

To study the effects of acid treatment on MWCNTs, FT-IR analysis was employed. Fig. 3 depicts FTIR spectra of the pure and modified MWCNTs. The FTIR spectrum of the pure MWCNTs displays a characteristic peak at 3,426 $cm^{-1}$ which is attributed to the existence of -OH groups. Two peaks at wavenumbers of 3,000-2,800 $cm^{-1}$ correspond to the -CH stretching. The peak at 1,632 $cm^{-1}$ is assigned to the C=C bond of carbon structure in MWCNTs. Besides, a peak at about 1,160 $cm^{-1}$ is related to the C-C bonds [34]. Comparison of the IR spectrum of the modified MWCNTs to that of

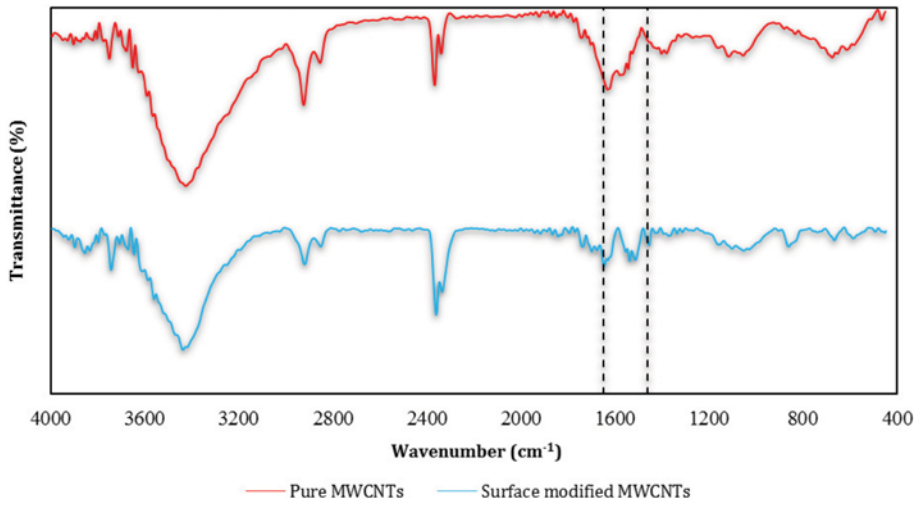


**Fig. 3. FTIR spectra of the neat MWCNTs and the surface modified MWCNTs.**

the neat MWCNTs reveals that several changes in functional groups of MWCNTs take place. For example, the peaks at 1,650 $cm^{-1}$ and 1,460 $cm^{-1}$ which characterize the carbonyl and carboxyl groups, respectively, confirm the effect of acid treatment on MWCNTs. Grafting of more chemical sites such as carboxyl groups onto the modified MWCNTs surface increases adsorption capacity of these nanoparticles and also creates an electrostatic stability required for better dispersion of the nanoparticles [24,35].

1-2-2. Membranes ATR-FTIR

Effects of surface modified MWCNTs addition into different grades of Pebax matrices were also investigated using ATR-FTIR spectra of the neat Pebax, and the Pebax nanocomposite membranes loaded with 1.5 and 2.5 wt% MWCNTs, as can be seen in Fig. 4.

ATR-FTIR spectrum of the neat Pebax 1074 demonstrates a peak at 1,112 $cm^{-1}$ which belongs to the stretching vibration of the ether group, C-O-C, in PE segment of Pebax. The peaks at 1,626 and 1,636 $cm^{-1}$ are assigned to the bonded and free stretching vibration of C=O group in H-N-C=O. The presence of O-C=O group is detectable with a peak at 1,734 $cm^{-1}$ in the hard segment. The bonded and free bending vibrations of N-H group in the PA block can be distinguished with two peaks at 1,548 and 1,564 $cm^{-1}$, respectively. Moreover, the double peaks at 3,290 and 3,328 $cm^{-1}$ are related to the stretching vibrations of hydrogen-bonded N-H and non-hydrogen-bonded N-H groups in Pebax 1074, respectively. In addition, the peaks at 2,922 and 1,460 $cm^{-1}$ represent the bending and stretching vibrations of C-H aliphatic bond, respectively [29,36,37].

As shown in Fig. 4, for the neat Pebax 1657 membrane, the symmetric vibration of the ether group, C-O-C, in the PE segment is characterized by a significant peak at 1,112 $cm^{-1}$. The peaks at 1,630 and 1,664 $cm^{-1}$ are attributed to the bonded and free stretching

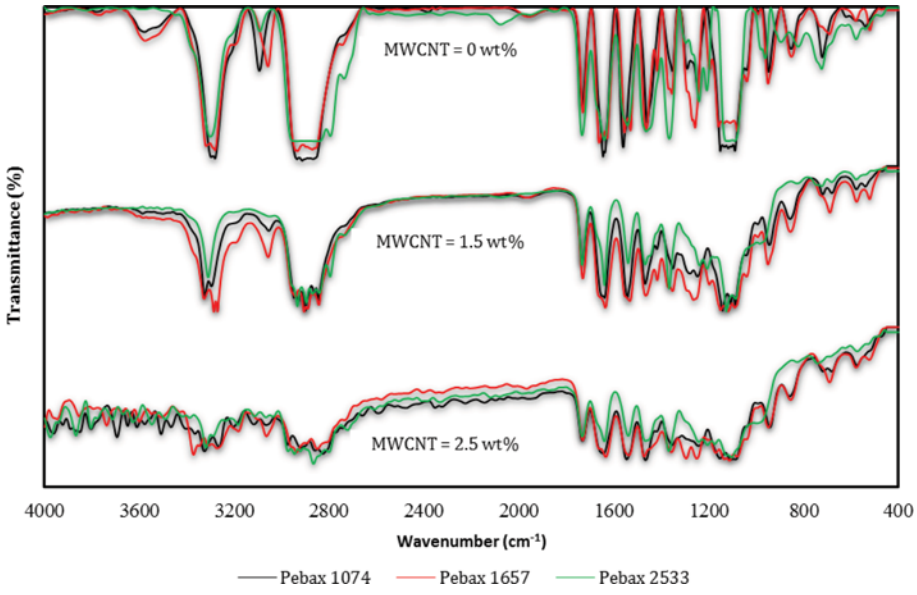


**Fig. 4. ATR-FTIR spectra of the fabricated membranes with different grades of Pebax and different loadings of MWCNTs.**

vibration of C=O group in H-N-C=O and the peak at 1,730 $cm^{-1}$ is related to the O-C=O group in the PA segment. The observed peaks at 1,548 and 1,564 $cm^{-1}$ are assigned to the bonded and free bending vibrations of N-H group in the PA segment, respectively. Besides, their stretching vibrations can be distinguished with peaks at 3,282 and 3,292 $cm^{-1}$. Furthermore, the most characteristic peaks at 2,856-2,948 and 1,464 $cm^{-1}$ show the existence of bending and stretching vibrations of C-H aliphatic group, respectively [29,36,37].

For the neat Pebax 2533 membrane, all the characteristic peaks that were observed in the ATR-FTIR spectra of the two other Pebax grades can be detected but with different positions. The characteristic peaks at 1,640 and 1,106 $cm^{-1}$ are attributed to the symmetric stretching vibration of amide (H-N-C=O) and ether (-C-O-C-) groups, respectively. The N-H stretching in the PA segment can be characterized by a peak at 3,300 $cm^{-1}$. Furthermore, there are two peaks around 2,850-2,950 $cm^{-1}$, which display the bending vibration of C-H stretch [38-40].

Comparison of ATR-FTIR spectra of the three types of nanocomposite membranes with those of the neat membranes shows that approximately the most signals corresponding to the neat Pebax functional groups can be observed in the Pebax membranes loaded with 1.5 and 2.5 wt% MWCNTs. However, there are some differences between the neat and the nanocomposite membranes when their spectra are examined carefully. As illustrated in Fig. 4, incorporation of MWCNTs into the Pebax matrices makes characteristics peaks at 2,910, 2,906 and 2,905 $cm^{-1}$ which are related to the C-H stretching of MWCNTs in Pebax 1074, Pebax 1657 and Pebax 2533, respectively. The peak intensity of interchain hydrogen bonding at 3,438-3,678 $cm^{-1}$ decreases and shifts left to the higher wave numbers. This phenomenon can be a proof of the membrane crystallinity reduction resulting from the interchain hydrogen bonding disruption. As can also be observed, positions of the mentioned peaks are altered more for Pebax 1074 compared to the two other Pebax grades, since it contains more PA segments (45%) and thus it can be influenced more by rupture of the interchain hydrogen bonding between PA segments. The ATR-FTIR results are in good agreement with the XRD results as described earlier [34,41,42].

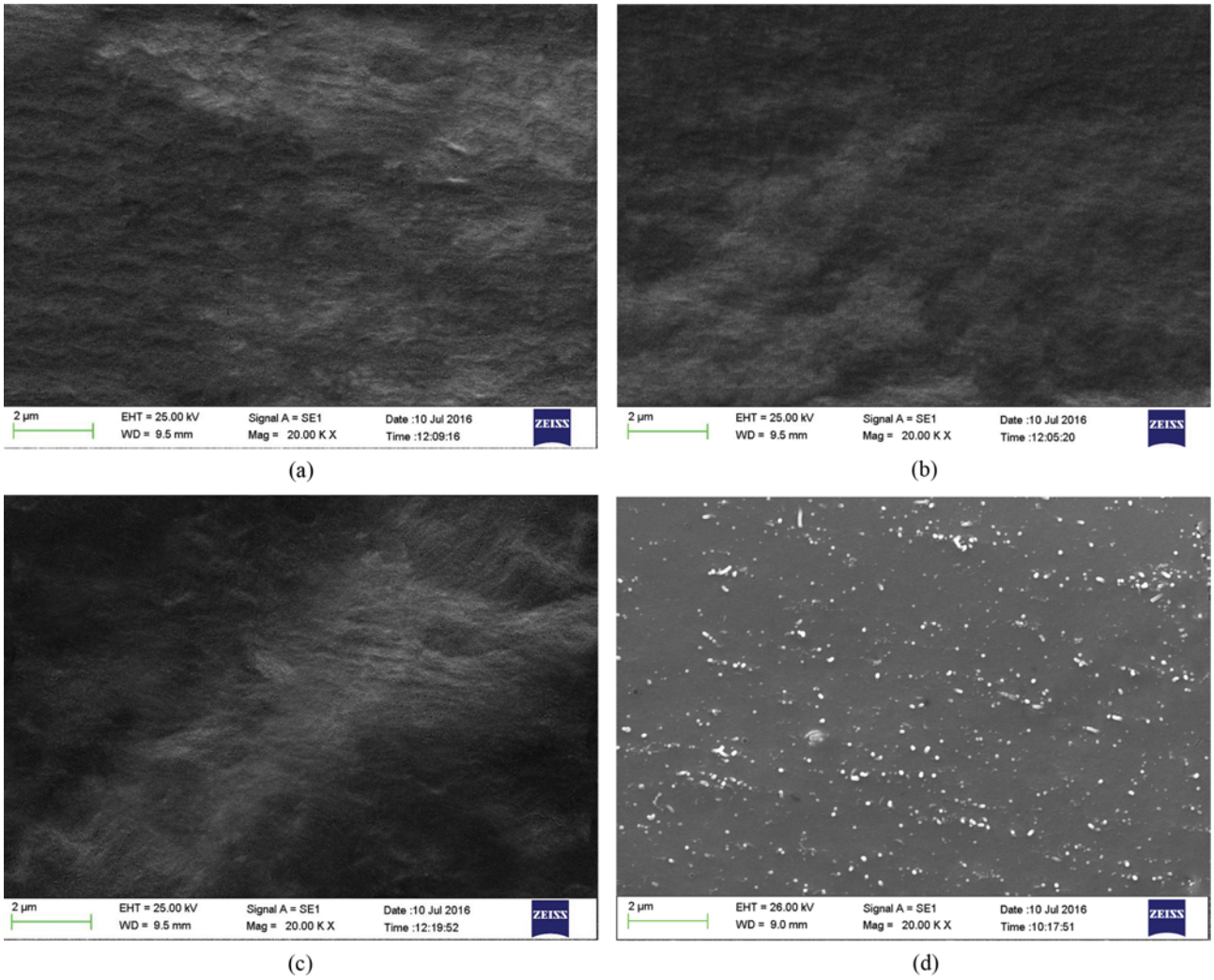


**Fig. 5. FESEM images of the fabricated membranes consisting of: (a) Neat Pebax 1074, (b) Neat Pebax 1657, (c) Neat Pebax 2533, (d) Pebax 1074 /MWCNT=1.5 wt%, (e) Pebax 1657/MWCNT=1.5 wt%, (f) Pebax 2533/MWCNT=1.5 wt%, (g) Pebax 1074/MWCNT=2.5 wt%, (h) Pebax 1657/MWCNT=2.5 wt%, (i) Pebax 2533/MWCNT=2.5 wt%.**

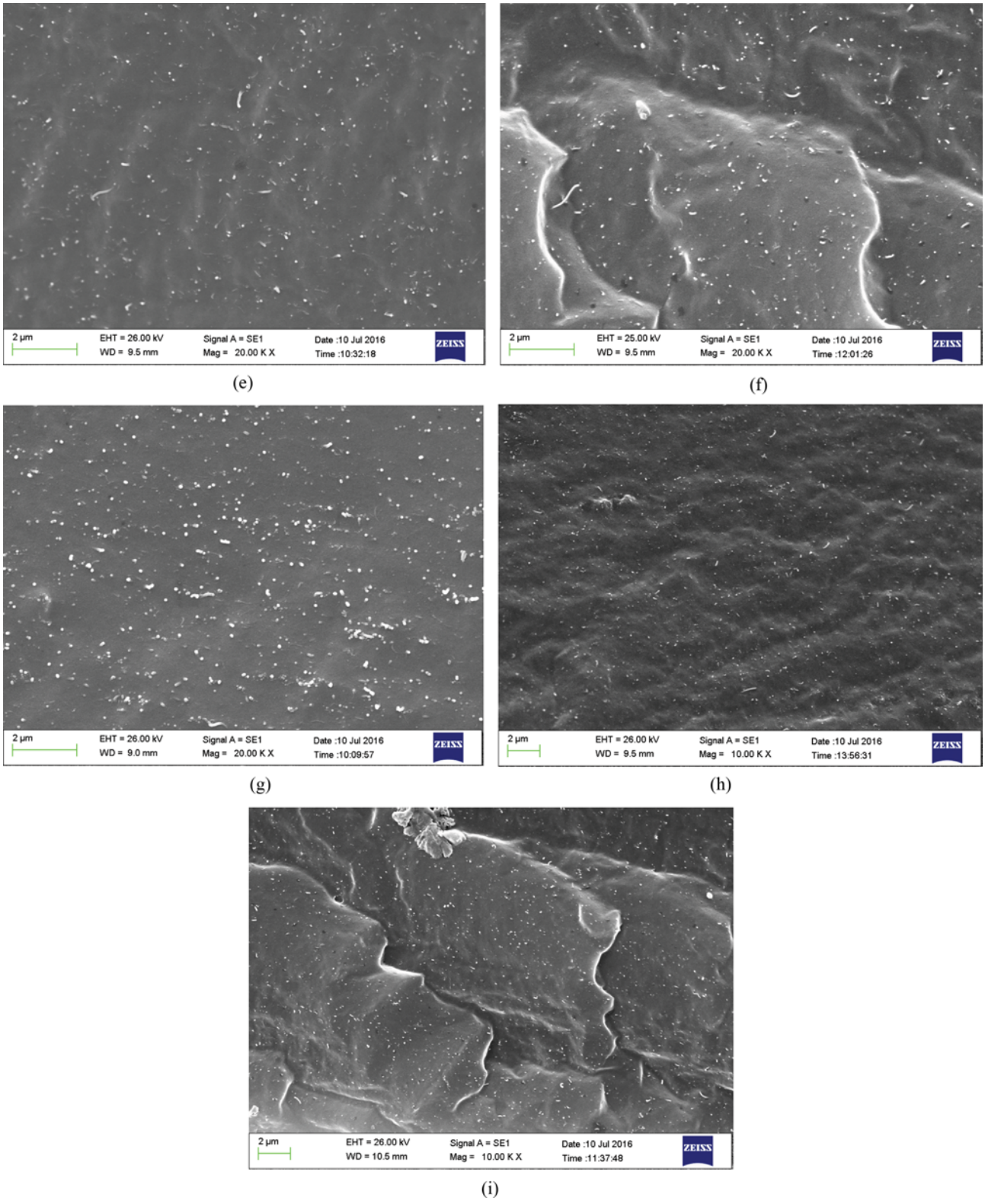


**Fig. 5. Continued.**

1-3. FESEM

Gas permeation is strongly influenced by the morphology of membranes. Therefore, investigation of the morphology using FESEM analysis is vital. FESEM images of the fabricated membranes with different grades of Pebax and different amounts of MWCNTs are presented in Fig. 5(a)-(i). According to Fig. 5(a), (b) and (c), cross-sectional morphology of the neat membranes (1074, 1657 and 2533) are uniform and they have fully dense structures

without any special defects. FESEM micrographs were investigated to study existence, distribution, agglomeration and phase separation of the nanoparticles. As illustrated in Fig. 5(d)-(i), uniform distribution of MWCNTs in the Pebax matrices was obtained without any significant cavities at the Pebax-MWCNTs interfaces. FESEM images demonstrated that the modified MWCNTs were in nanometer scale after distribution in the polymers matrices. According to the images, the lighter region is related to the MWCNTs and the darker part is attributed to the Pebax matrices [43,44].

The major reason why nanoparticles tend to be agglomerated in polymer matrices is the significant difference of surface energies between nanoparticles and polymers. Sedimentation and agglomeration of nanoparticles are attributed to high attractive energy between the nanoparticles. Therefore, for good distribution of the nanoparticles in the polymer matrices, these energies must be reduced and balanced by a kind of modification [43,44]. In this study, surface modification of MWCNTs was used before their incorporation into the polymer matrices. The combination of surface modification and powerful sonication could result in good dispersion of MWCNTs [1,45]. As observed in Fig. 5(d)-(f), the nanocomposite membranes containing 1.5 wt% MWCNTs have uniform MWCNTs distributions. However, the modified MWCNTs tend to be slightly agglomerated in matrices of the Pebax nanocomposite membranes as the nanoparticle loading increases. This can be observed in FESEM images of the nanocomposite membranes containing 2.5 wt% MWCNTs (Fig. 5(g)-(i)). However, the agglomeration of the modified nanoparticles in the polymer matrices is not considerable [46].

**2. Gas Permeation Properties**

2-1. Effect of MWCNTs Loadings

Effect of MWCNTs content on $CO_2$ and $CH_4$ permeability and also ideal $CO_2/CH_4$ selectivity values of the prepared nanocomposite membranes with different Pebax grades temperature of at 25 °C and pressure of 2 bar is presented in Fig. 6(a), (b) and (c). As observed, with increasing the MWCNTs content, permeability of $CO_2$ and $CH_4$ gases in all the Pebax membranes (1074, 1657 and 2533) increases [34,45,47,48]. For instance, by increasing MWCNTs content from zero to 2.5 wt% in Pebax 1074 at the pressure of 2 bar, $CO_2$ permeability increases from 60.85 to 134.25 Barrer. Besides, at the same conditions, $CH_4$ permeability increases from 3.20 to 6.47 Barrer. Moreover, for the Pebax 1657 based nanocomposite membranes, $CO_2$ permeability changes from 67.18 to 137.34 Barrer and $CH_4$ permeability increases from 3.67 to 7.16 Barrer. The corresponding changes for the Pebax 2533 based nanocomposite membranes are from 196.32 to 243.85 Barrer for $CO_2$ and from 27.09 to 33.28 Barrer for $CH_4$.

The amount of PE units in various grades of Pebax are different and these differences influence the crystallinity and d-spacing values of the prepared membranes. As mentioned, the less crystallinity and the bigger d-spacing value, the higher gas permeability value [32,33,46]. Since the order of crystallinity of three types of the neat membranes is Pebax 2533<Pebax 1657<Pebax 1074 and that of the d-spacing is as Pebax 2533>Pebax 1657>Pebax 1074, the order of both gases' permeabilities through the neat membranes presents as Pebax 2533>Pebax 1657>Pebax 1074 [1,33]. Additionally, $CO_2$ permeability is higher than $CH_4$ through all the three neat

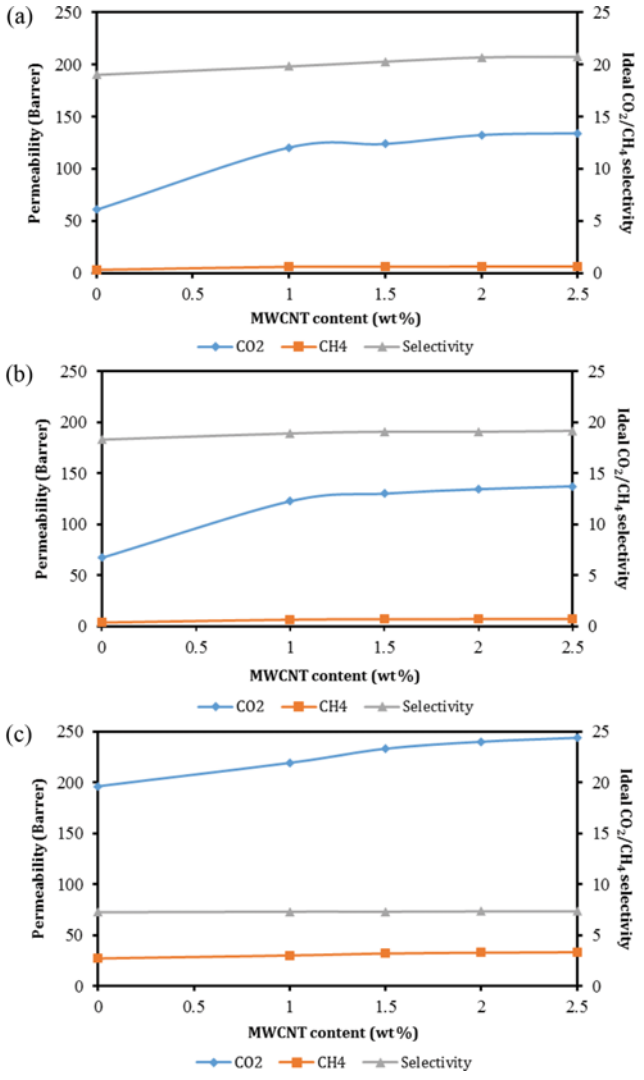


**Fig. 6. Effect of MWNTs content on $CO_2$ and $CH_4$ permeabilities and $CO_2/CH_4$ ideal selectivity of the fabricated membranes with different grades of Pebax and different loadings of MWCNTs at 25 °C and 2 bar, (a) Pebax 1074, (b) Pebax 1657 and (c) Pebax 2533.**

membranes because its affinity to PE segments is more than $CH_4$ [36,46]. The addition of nanoparticles into polymers can also affect crystallinity of the prepared membranes. As observed in the XRD patterns, incorporation of MWCNTs leads to crystallinity decrement due to the reduction of interchain hydrogen bondings between the PA segments. Furthermore, because of incompatibility between MWCNTs and Pebax matrices, the formation of some voids in the nanoparticles-Pebax interfaces is inevitable. The combination of crystallinity reduction and voids formation results in gas permeability increment. Therefore, both gases' permeabilities increase with increasing MWCNTs content [34,45].

The results from previous studies showed that capacity adsorption of MWCNTs to $CO_2$ is higher than that to $CH_4$ [1,21]. Hence, as expected, $CO_2$ permeability through the prepared nanocomposite membranes increases more than $CH_4$ as MWCNTs content increases due to the more adsorption sites of MWCNTs. Conse-

quently, with increasing MWCNTs content, ideal $CO_2/CH_4$ selectivity increases owing to the higher affinity of $CO_2$ to MWCNTs [1,46]. For example, at pressure of 2 bar and temperature of 25 °C, with increasing MWCNTs content from 0 to 2.5 wt%, ideal $CO_2/CH_4$ selectivity of the prepared nanocomposite membrane with Pebax 1074 increases from 19.01 to 20.74 (9.1% increase). Similarly, the selectivity values for Pebax 1657 and Pebax 2533 nanocomposite membranes increase from 18.32 to 19.17 (4.6% increase) and from 7.25 to 7.33 (1.1% increase), respectively. A seen, the ideal $CO_2/CH_4$ selectivity of Pebax 1074 nanocomposite membrane is influenced more than the two other nanocomposite membranes by increasing MWCNTs content. This can be due to the higher content of PA blocks in Pebax 1074 membrane which are connected by interchain hydrogen bondings, and accordingly incorporation of MWCNTs in Pebax 1074 based membrane may disrupt these bondings more than the bondings in the two other Pebax based membranes.

2-2. Effect of Feed Pressure

Pressure can affect gas permeability through the membranes in several respects. First, increasing pressure can cause the membranes to be compacted more, and it can result in a reduction of FFV and consequently gas diffusion. In fact, as feed pressure increases, the volume of a polymeric membrane (V) decreases due to its polymer chains packing, and consequently fractional free volume of the membrane decreases based on its definition ($FFV=1-(V_0/V)$). There is also a good correlation between FFV and diffusion coefficient of a penetrant ($D=Aexp(-(\gamma v^*/FFV))$). As seen in the equation (Cohene-Turnbull model), the diffusion coefficient decreases as FFV decreases. Second, it acts as driving force for gas transport

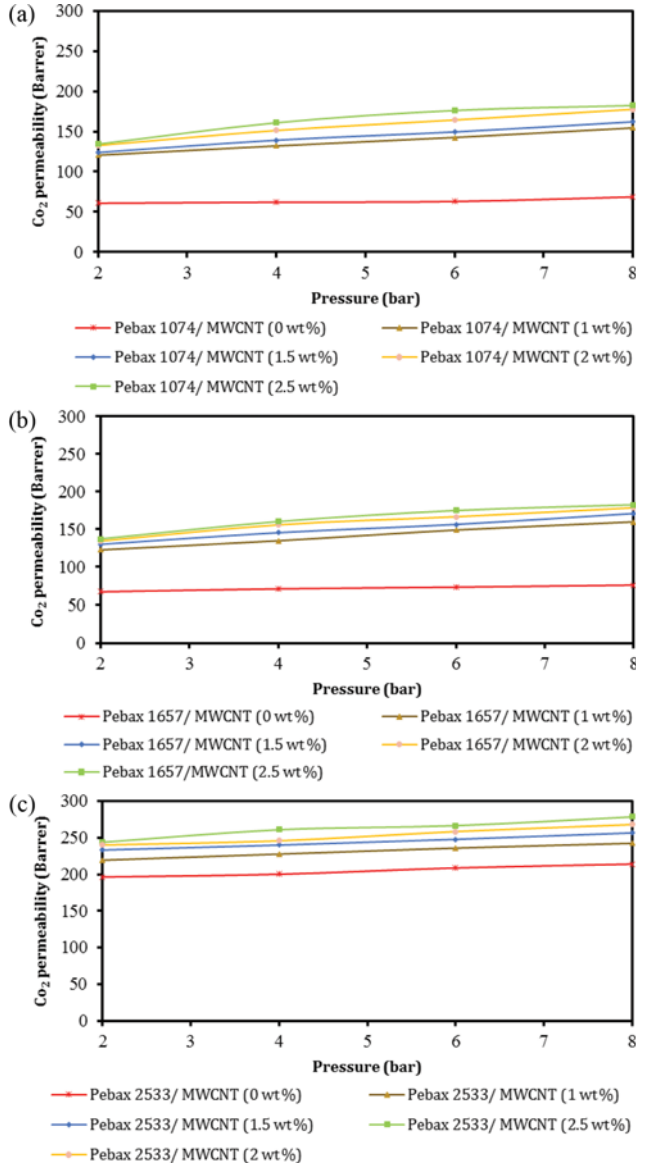


**Fig. 7. Effect of feed pressure on $CO_2$ permeability of the fabricated membranes with different grades of Pebax and different loadings of MWCNTs, (a) Pebax 1074, (b) Pebax 1657 and (c) Pebax 2533.**

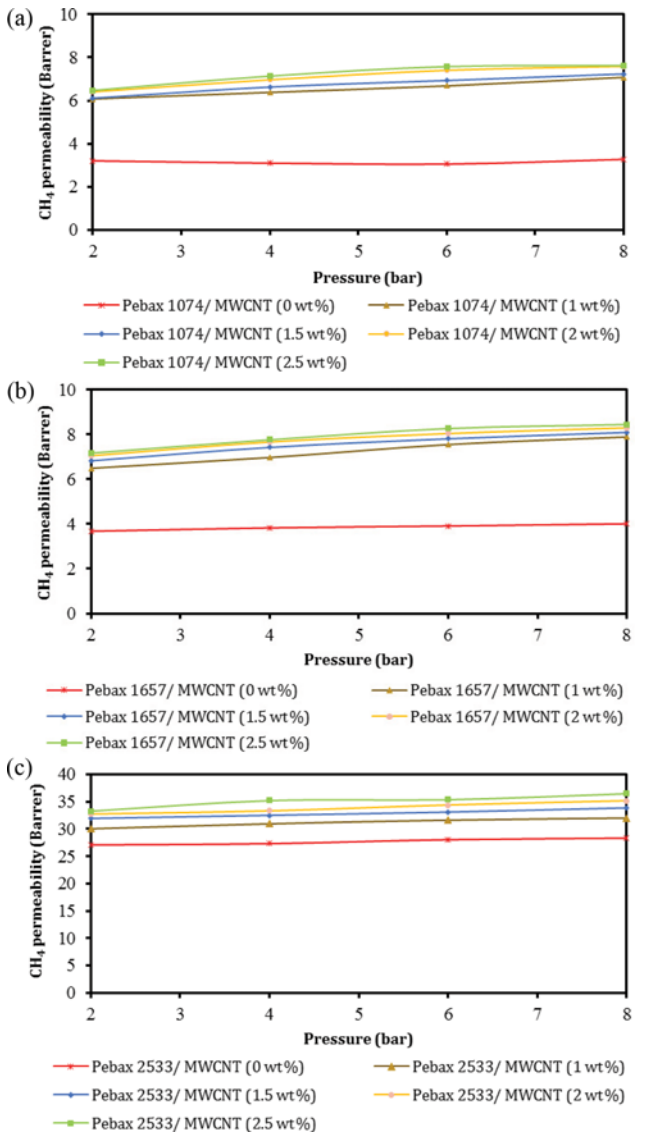


**Fig. 8. Effect of feed pressure on $CH_4$ permeability of the fabricated membranes with different grades of Pebax and different loadings of MWCNTs, (a) Pebax 1074, (b) Pebax 1657 and (c) Pebax 2533.**

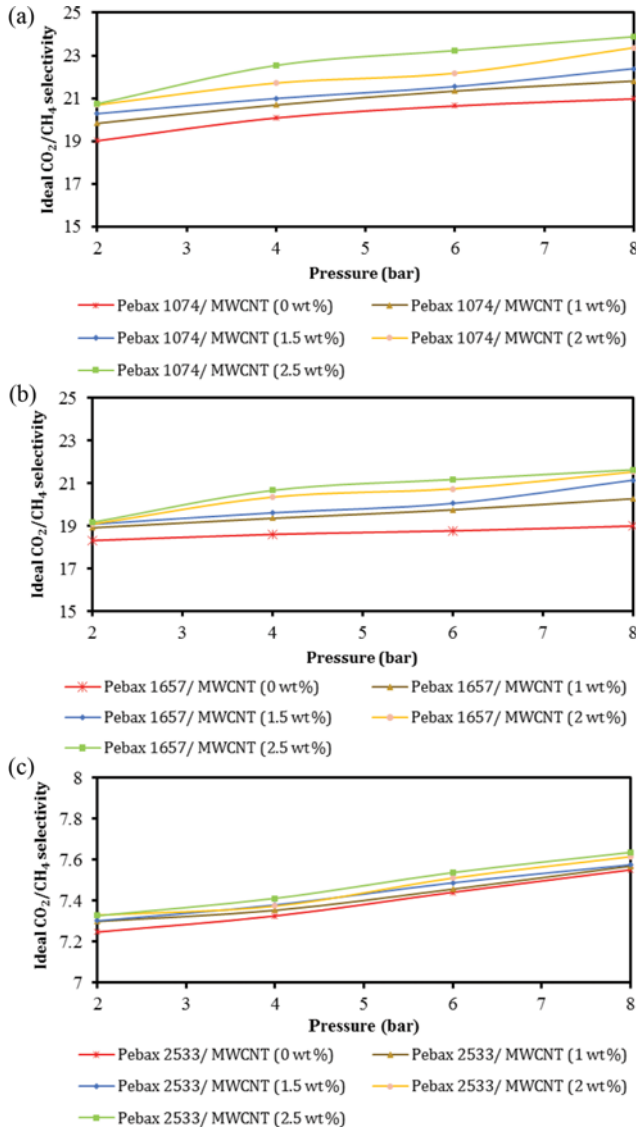


**Fig. 9. Effect of feed pressure on $CO_2/CH_4$ ideal selectivity of the fabricated membranes with different grades of Pebax and different loadings of MWCNTs, (a) Pebax 1074, (b) Pebax 1657 and (c) Pebax 2533.**

through the membranes. Third, the solubility of gases is enhanced owing to increasing gas concentration resulting from pressure increment, and since gas permeability coefficient is the multiplication of diffusion and solubility, gas permeation can increase when solubility coefficient increases [37,49].

Effects of feed pressure (from 2 to 8 bar) on the performance of the synthesized membranes were investigated as illustrated in Figs. 8-10. Increasing the feed pressure increases $CO_2$ and $CH_4$ permeability and also ideal $CO_2/CH_4$ selectivity values for all the membranes. As an example, by increasing pressure from 2 to 8 bar, $CO_2$ permeability values for Pebax 1074, Pebax 1657 and Pebax 2533 nanocomposite membranes with MWCNTs content of 2.5 wt% improve from 134.25 to 182.24 Barrer, 137.34 to 182.64 Barrer and 243.85 to 278.43 Barrer, respectively. Also, $CH_4$ permeability values increase from 6.47 to 7.63 Barrer, 7.16 to 8.44 Barrer and 33.28

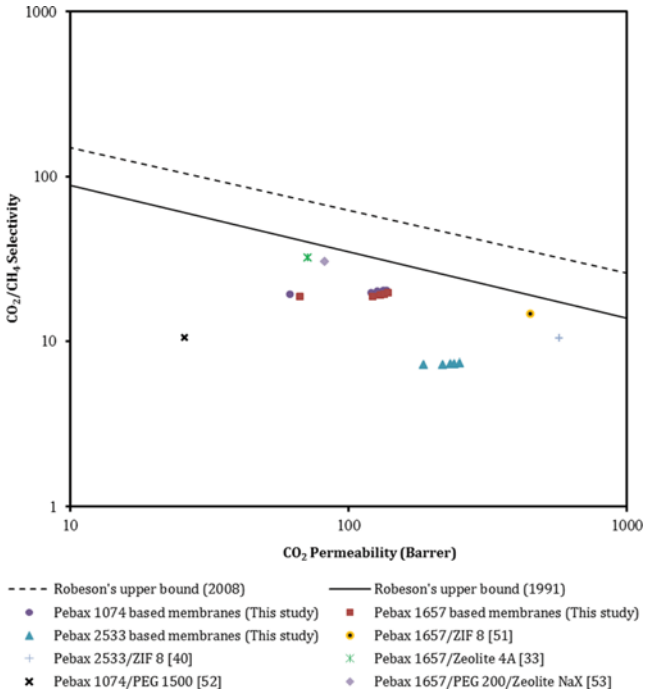


**Fig. 10. Comparison of $CO_2/CH_4$ separation performance of the fabricated membranes with the Robeson's upper bound limits.**

to 36.46 Barrer for the nanocomposite membranes loaded with the same MWCNTs content, respectively. According to permeability coefficient definition, the increment in both gases permeabilities is mainly due to the enhancement of driving force for gas transfer. This increment can also be due to the higher gas concentration (solubility) [1,46].

Furthermore, ideal $CO_2/CH_4$ selectivity of gases enhances from 20.74 to 23.88, 19.17 to 21.63 and 7.33 to 7.64 for the prepared membranes with 1074, 1657 and 2533 Pebax grades at the same conditions, respectively. Since $CO_2$ is a condensable gas with great affinity to PE segment compared to $CH_4$ and it has lower kinetic diameter (3.3 Å) than $CH_4$ (3.8 Å), its permeability through the prepared membranes is higher than $CH_4$ [46]. Besides, for the nanocomposite membranes, $CO_2$ adsorption capacity of MWCNTs increases as feed pressure increases. Additionally, $CO_2$ permeability can increase more due to the plasticization effect which is related to the nature of $CO_2$ [50].

As mentioned earlier, three grades of Pebax have different polyether content (55, 60 and 80 for Pebax 1074: 55%, Pebax 1657: 60% and Pebax 2533: 80%). Since PE content is responsible for gas permeability through the Pebax based membranes, with increasing pressure as driving force, the order of gases' ($CO_2$ and $CH_4$) permeabilities through the membranes is as: Pebax 2533>Pebax 1657> Pebax 1074. On the other hand, The XRD and FT-IR results showed that the MWCNTs incorporation into the polymers matrices can influence the Pebax 1074 based membrane more than the two other membranes as it has higher PA content. This segment (PA), which is responsible for mechanical strength of the membranes and plays a role as a barrier for gas transfer through the membranes, can be reduced due to the nanoparticles incorporation re-

sulting from rupture of hydrogen bonding between the PA segments. It means crystallinity of the Pebax 1074 can be reduced more due to the MWCNTs incorporation; therefore, for a constant loading of MWCNTs in the Pebax based membranes, the gases, particularly $CO_2$, can diffuse more easily through the Pebax 1074/MWCNT nanocomposite membrane with increasing pressure. As a result, ideal $CO_2/CH_4$ selectivity of the Pebax 1074/MWCNT membrane changes more as feed pressure increases.

**3. Comparison of the Results with the Robeson's Upper Bound Limits**

A standard approach for the analysis of gas separation membranes is a consideration of data points in selectivity-permeability plots (so-called Robeson diagrams). The endeavor of researchers is to approach the bound limits in these diagrams (Robeson's upper bound lines) which was first proposed in 1991 [7] and then presented in 2008 [8]. To compare gas separations results of this work with the Robeson's upper bound lines, the prepared membranes properties at the temperature of 25 °C and pressure of 2 bar are presented in Fig. 10.

As indicated, the performance of the prepared membranes with Pebax 1074 and Pebax 1657 as the basic polymers is closer to Robeson's upper bound limits compared to the prepared Pebax 2533 based membranes, and this performance is even better for the Pebax 1074 membranes in comparison with the Pebax 1657 membranes. Besides, the performance improves with increasing MWCNTs content. In other words, the position of the prepared nanocomposite membranes data points is closer to the Robeson's upper bound limits compared to that of the neat membranes.

To analyze the results more, the performance of other Pebax based nanocomposite membranes was collected as presented in Table 3 [33,40,51-53]. As observed, ideal $CO_2/CH_4$ selectivity of the prepared Pebax 1074 nanocomposite membranes containing 2.5 wt% of MWCNTs is higher than that of the other Pebax based nanocomposite membranes prepared by other researchers.

## CONCLUSION

Three different Pebax grades (Pebax 1657, Pebax 1074 and Pebax 2533) were selected as the basic materials and MWCNTs as the nanofillers for synthesis of polymeric membranes. Pebax 1657/MWCNTs, Pebax 1074/MWCNTs and Pebax 2533/MWCNTs nanocomposite membranes with different loadings of MWCNTs (1-2.5 wt%) were synthesized for $CO_2/CH_4$ separation. MWCNTs nanofillers were surface modified before incorporating into the polymers matrices. To investigate the effect of the nanofillers loading on performance of the prepared membranes, permeation values of $CO_2$ and $CH_4$ gases through the membranes were measured. The results revealed that all the synthesized nanocomposite membranes exhibited better gas permeation properties than those of the three neat Pebax membranes under the same conditions. With increasing the nanofillers content, both $CO_2$ and $CH_4$ gases permeability values increased. Ideal $CO_2/CH_4$ selectivity was higher for the Pebax 1074/MWCNTs nanocomposite membrane with 2.5 wt% MWCNTs loading. Cross-sectional FESEM micrographs of all the three types of nanocomposite membranes with different loadings of MWCNTs showed the uniform dispersion of the nanofillers at lower loadings. However, agglomeration tendency of the nanofillers was observed at the highest loadings (2.5 wt%). FESEM images also revealed that the membranes had dense structures where the nanofillers do not exist. Chemical bonds changes of the synthesized membranes were examined using ATR-FTIR analysis. ATR-FTIR spectra of the synthesized membranes exhibited that the wavenumbers and the intensities of some peaks for the neat Pebax membranes changed with increasing MWNCTs content due to disruption of the interchain hydrogen bonding between the PA segments of the polymers. Structural characterization of the synthesized membranes was also carried out using XRD analysis. The XRD results showed that the diffraction peaks in the crystalline region of different grades of Pebax decreased with increasing the nanofiller content in the polymers matrices. The reduction in crystalline nature of the polymers can also be due to the rupture of interchain hydrogen bonding between the PA segments. As seen, the XRD results are completely in good agreement with the ATR-FTIR results. Also, a comparison between permeability-selectivity values of the prepared nanocomposite membranes and the Robeson's diagram showed the potential of Pebax/MWCNTs nanocomposite membranes for $CO_2/CH_4$ separation in natural gas sweetening due to their improved separation properties.

## REFERENCES

1. D. Zhao, J. Ren, H. Li, X. Li and M. Deng, *J. Membr. Sci.*, **467**, 41 (2014).
2. J. K. Adewole and A. L. Ahmad, *Korean J. Chem. Eng.*, **33**, 2998 (2016).
3. M. T. Ravanchi, S. Sahebdelfar and F. T. Zangeneh, *Front. Chem. Sci. Eng.*, **5**, 173 (2011).
4. W. Yave, A. Car and K. V. Peinemann, *J. Membr. Sci.*, **350**, 124 (2010).
5. A. Car, C. Stropnik, W. Yave and K.-V. Peinemann, *Sep. Purif. Technol.*, **62**, 110 (2008).

**Table 3. Comparison of this work results with the other published results**

| Membrane type | Filler content (wt%) | Pressure (bar) | Temperature (°C) | $P_{CO_2}$ (Barrer) | $\alpha_{CO_2/CH_4}$ | Ref. |
|---|---|---|---|---|---|---|
| Pebax 1657/ZIF 8 | --- | 2 | 25 | 449 | 14.7 | [51] |
| Pebax 2533/ZIF 8 | 15 | 2 | 25 | 574 | 10.4 | [40] |
| Pebax 1657/Zeolite 4A | 5 | 5 | 25 | 71.4 | 32.2 | [33] |
| Pebax 1074/PEG 1500 | 30 | 5 | 35 | 25.7 | 10.6 | [52] |
| Pebax 1657/PEG 200/ Zeolite NaX | 30 | 2 | 25 | 82.2 | 30.5 | [53] |
| Pebax 1074/MWCNT | 2.5 | 2 | 25 | 134.2 | 20.7 | This study |

6. N. Azizi, T. Mohammadi and R. M. Behbahani, *J. Energy Chem.*, (2017).
7. L. M. Robeson, *J. Membr. Sci.*, **62**, 165 (1991).
8. L. M. Robeson, *J. Membr. Sci.*, **320**, 390 (2008).
9. L. Robeson, B. Freeman, D. Paul and B. Rowe, *J. Membr. Sci.*, **341**, 178 (2009).
10. M. A. Semsarzadeh, B. Ghalei, M. Fardi, M. Esmaeeli and E. Vakili, *Korean J. Chem. Eng.*, **31**, 841 (2014).
11. F. Peng, L. Lu, H. Sun, Y. Wang, H. Wu and Z. Jiang, *J. Membr. Sci.*, **275**, 97 (2006).
12. M. Sadeghi, H.T. Afarani and Z. Tarashi, *Korean J. Chem. Eng.*, **32**, 97 (2015).
13. D. Zhao, J. Ren, H. Li, K. Hua and M. Deng, *J. Energy Chem.*, **23**, 227 (2014).
14. H. Lin and B. D. Freeman, *J. Mol. Struct.*, **739**, 57 (2005).
15. N. Azizi, T. Mohammadi and R. M. Behbahani, *J. Nat. Gas. Sci. Eng.*, **37**, 39 (2017).
16. A. Jomekian, R. M. Behbahani, T. Mohammadi and A. Kargari, *Korean J. Chem. Eng.*, **34**, 440 (2017).
17. S. Kim, L. Chen, J. K. Johnson and E. Marand, *J. Membr. Sci.*, **294**, 147 (2007).
18. F. H. Akhtar, M. Kumar and K.-V. Peinemann, *J. Membr. Sci.*, **525**, 187 (2017).
19. D. Zhao, J. Ren, Y. Wang, Y. Qiu, H. Li, K. Hua, X. Li, J. Ji and M. Deng, *J. Membr. Sci.*, **521**, 104 (2017).
20. A. Jomekian, B. Bazooyar, R. M. Behbahani, T. Mohammadi and A. Kargari, *J. Membr. Sci.*, **524**, 652 (2017).
21. E. Molyanyan, S. Aghamiri, M. R. Talaie and N. Iraji, *Int. J. Environ. Sci. Technol.*, **13**, 2001 (2016).
22. Y.-C. Tsai and J.-D. Huang, *Electrochem. Commun.*, **8**, 956 (2006).
23. Z. Es'haghi, M. A. Golsefidi, A. Saify, A. A. Tanha, Z. Rezaeifar and Z. Alian-Nezhadi, *J. Chromatogr. A*, **1217**, 2768 (2010).
24. J. Shen, W. Huang, L. Wu, Y. Hu and M. Ye, *Mater. Sci. Eng. A*, **464**, 151 (2007).
25. N. Azizi, T. Mohammadi and R. Mosayebi Behbahani, *Chem. Eng. Res. Des.*, **117**, 177 (2017).
26. M. Isanejad, N. Azizi and T. Mohammadi, *J. Appl. Polym. Sci.*, **134** (2017).
27. H. R. Mahdavi, N. Azizi and T. Mohammadi, *J. Polym. Res.*, **24**, (2017).
28. S. A. Stern, *J. Polym. Sci. A. Polym. Phys.*, **6**, 1933 (1968).
29. J. H. Kim and Y. M. Lee, *J. Membr. Sci.*, **193**, 209 (2001).
30. A. F. Ismail, K. C. Khulbe and T. Matsuura, *Gas Separation Membranes: Polymeric and Inorganic*, Springer International Publishing, Cham (2015).
31. S. Sridhar, R. Suryamurali, B. Smitha and T. M. Aminabhavi, *Colloid. Surf., A. Phys. Eng. Aspects*, **297**, 267 (2007).
32. S. Sridhar, B. Smitha, R. Suryamurali and T. M. Aminabhavi, *Des. Mono. Polym.*, **11**, 17 (2008).
33. R. Surya Murali, A. F. Ismail, M. A. Rahman and S. Sridhar, *Sep. Purif. Technol.*, **129**, 1 (2014).
34. R. S. Murali, S. Sridhar, T. Sankarshana and Y. Ravikumar, *Ind. Eng. Chem. Res.*, **49**, 6530 (2010).
35. P. Zaheri, T. Mohammadi, H. Abolghasemi and M. G. Maraghe, *Chem. Eng. Res. Des.*, **100**, 81 (2015).
36. A. Ghadimi, M. Amirilargani, T. Mohammadi, N. Kasiri and B. Sadatnia, *J. Membr. Sci.*, **458**, 14 (2014).
37. H. Rabiee, A. Ghadimi, S. Abbasi and T. mohammadi, *Chem. Eng. Res. Des.*, **98**, 96 (2015).
38. A. Ehsani and M. Pakizeh, *J. Taiwan. Instit. Chem. Eng.*, **66**, 414 (2016).
39. M. C. Choi, J. Y. Jung, H. S. Yeom and Y. W. Chang, *Polym. Eng. Sci.*, **53**, 982 (2013).
40. V. Nafisi and M.-B. Hägg, *J. Membr. Sci.*, **459**, 244 (2014).
41. B. Yu, H. Cong, Z. Li, J. Tang and X. S. Zhao, *J. Appl. Polym. Sci.*, **130**, 2867 (2013).
42. D. Zhao, J. Ren, H. Li, X. Li and M. Deng, *J. Membr. Sci.*, **467**, 41 (2014).
43. M. Rezakazemi, A. Vatani and T. Mohammadi, *RSC Adv.*, **5**, 82460 (2015).
44. H. Rabiee, S. Meshkat Alsadat, M. Soltanieh, S. A. Mousavi and A. Ghadimi, *J. Indust. Eng. Chem.*, **27**, 223 (2015).
45. H. Cong, J. Zhang, M. Radosz and Y. Shen, *J. Membr. Sci.*, **294**, 178 (2007).
46. S. Wang, Y. Liu, S. Huang, H. Wu, Y. Li, Z. Tian and Z. Jiang, *J. Membr. Sci.*, **460**, 62 (2014).
47. L. Ge, Z. Zhu, F. Li, S. Liu, L. Wang, X. Tang and V. Rudolph, *J. Phys. Chem. C.*, **115**, 6661 (2011).
48. S. Habibzare, M. Asghari and A. Djirsarai, *Int. J. Nano. Dimension*, **5**, 247 (2014).
49. H. Rabiee, A. Ghadimi and T. Mohammadi, *J. Membr. Sci.*, **476**, 286 (2015).
50. D. W. Van Krevelen and K. Te Nijenhuis, *Properties of Polymers*, Elsevier, Amsterdam (2009).
51. A. Jomekian, R. M. Behbahani, T. Mohammadi and A. Kargari, *J. Nat. Gas. Sci. Eng.*, **31**, 562 (2016).
52. S. Feng, J. Ren, K. Hua, H. Li, X. Ren and M. Deng, *Sep. Purif. Technol.*, **116**, 25 (2013).
53. A. Mahmoudi, M. Asghari and V. Zargar, *J. Indust. Eng. Chem.*, **23**, 238 (2015).
54. A. Fonseca, S. Reijerkerk, J. Potreck, K. Nijmeijer, Z. Mekhalif and J. Delhalle, *Desalination*, **250**, 1150 (2010).